ROYAL SOCIETY
OF CHEMISTRY

PAPER

Selective transesterification mediated by lanthanum complexes in the copolymerisation of lactide and δ-valerolactone†

Richard J. Pearcy,[a] Stuart R. Berrow [ID] [b] and Rachel H. Platel [ID] *[a]

Poly(lactide-*co*-valerolactone) copolymers were prepared *via* the one-pot copolymerisation of *rac*-lactide or *S,S*-lactide with δ-valerolactone at ambient temperature, mediated by bis(dimethylsilyl)amido lanthanum complexes supported by ligands derived from a salan framework (salan = *N,N′*-bis(*o*-hydroxy, *m*-di-*tert*-butylbenzyl)-1,2-diaminoethane), which incorporate either benzyl or 2-pyridyl groups at the tertiary amine moieties. Poly(δ-valerolactone)s were also prepared by the ring-opening polymerisation of δ-valerolactone and high molecular weight polymers (up to 83.6 kg mol^{-1}) with narrow dispersities were obtained. The poly(lactide-*co*-valerolactone) copolymers were fully characterized using ^{1}H and ^{13}C NMR spectroscopy, gel-permeation chromatography and differential scanning calorimetry. Both the reaction solvent (toluene or THF) and the number of 2-pyridyl groups the complex possesses affect the complex activity and copolymer microstructure. The use of a non-coordinating solvent and presence of at least one 2-pyridyl group is required for high conversion of both monomers. Variation of the monomer feed ratio allowed copolymers across the full compositional range to be prepared. The copolymers are formed *via* a transesterification mechanism whereby all of the lactide undergoes rapid polymerisation in the early stages of the reaction and the δ-valerolactone is subsequently incorporated into the polymer. The rate and extent of δ-valerolactone polymerisation increases with the number of 2-pyridyl groups in the catalyst in toluene and is more rapid in non-coordinating solvent (toluene) than coordinating solvent (THF). Only low levels of the T_{II} mode of transesterification occur, with the T_I transesterification mode dominating, leading to the formation of copolymers with intact lactidyl units.

Introduction

Biodegradable polymers are of increasing interest as the plastic waste crisis intensifies and materials that are accessible from renewable resources are

[a]Department of Chemistry, Lancaster University, Lancaster, LA1 4YB, UK. E-mail: r.platel@lancaster.ac.uk

[b]School of Physics and Astronomy, University of Leeds, Leeds, LS2 9JT, UK

sought.[1–4] Aliphatic polyesters have delivered diverse properties, along with the possibility of degradation, and/or the derivation from alternative sources to petroleum. These polymers find applications as commodity plastics,[5,6] in engineering and, due to their degradability *in vivo*, in medical applications.[7]

Polylactide (PLA) is an aliphatic polyester that derives from sugar beet or corn. It is prepared *via* the metal-initiated ring-opening polymerisation of the cyclic diester lactide (LA), comprising two lactic acid units, by a coordination–insertion mechanism.[8] Transesterification, the exchange of ester groups within the polymer chain,[9] is generally considered to be an undesirable side reaction, mediated by the catalyst, that competes with the ROP propagation reaction, especially at high temperatures and low monomer concentrations. It can occur inter- and intra-molecularly,[10] and results in a broadening of molecular mass distribution and reduction in molecular weight control.[11] PLA has a relatively high T_g of 57 °C and is very tough, however, it is also very brittle and relatively slow to undergo hydrolysis and degrade.[12,13] The presence of a methyl group in the lactic acid moiety offers the opportunity for stereocontrol in ROP when racemic monomer (a mixture of R,R-LA and S,S-LA) is used,[14] which allows for limited tuning of the polymer properties. For example, whilst atactic PLA is amorphous, poly(R-lactide) and poly(S-lactide) are crystalline with $T_m \sim 180$ °C, whilst stereoblock PLA can reach T_m of up to 230 °C.[15–17]

An alternative route to widen the accessible property window of a material is through copolymerisation with another monomer.[18] Depending on the sequential arrangement of the two monomer units in a polymer, block, statistical, gradient and alternating copolymers can be prepared. In a block copolymer, the properties of each homopolymer are maintained, whilst a statistical copolymer delivers a material whose properties are usually intermediate between the two parent homopolymers. In a metal catalysed one-pot ROP reaction, the inherent relative reactivities of each monomer usually dictate the resulting copolymer structure. This means that statistical copolymers are challenging to prepare and often gradient copolymers result.

Poly(δ-valerolactone) (PVL) has T_m of ~57 °C and T_g -53 °C.[19] High molecular weight PVL has excellent mechanical properties (including high tensile strength and excellent ductility). It is prepared from the ROP of δ-valerolactone (δ-VL), a 6-membered lactone. Compared to its seven-membered ring counterpart, ε-caprolactone (ε-CL), δ-VL is much less-well explored, particularly in its copolymerisation with LA.[18] However, the properties of PVL are complementary to those of PLA, making it a good choice as a comonomer.

The synthesis of poly(lactide-b-δ-valerolactone) block copolymers has been reported,[20,21] as well as metal-catalysed one-pot δ-VL and LA copolymerisation using tin,[22–25] aluminium[26] and lanthanide[27] catalysts. Generally, in a monomer mixture of LA and δ-VL, LA is found to have much greater reactivity than δ-VL. Recently, [La(OCH$_2$Ph)$_3$]$_x$ was reported as a catalyst to prepare high molecular weight PVL *via* the ROP of δ-VL under mild conditions, which displayed high thermal stability and excellent mechanical properties (high tensile strength, ductility and toughness), as well as facile depolymerisation back to monomer in the presence of a catalyst.[28] Additionally, the composition and copolymer architecture of a series of poly(lactide-co-valerolactone) copolymers, prepared using Sn(Oct)$_2$ with either salicylic acid or benzyl alcohol as the initiator, were shown to be key to the physical properties of the copolymers and degradation profiles

under composting conditions.[29] These studies highlight the relevance of PVL and δ-VL as a monomer, as well as the need for greater understanding of the potential of poly(lactide-*co*-valerolactone)s.

Transesterification can occur in copolymerisation reactions and can be used as a route to randomise monomer distribution, usually at elevated temperature.[30–33] Due to a ring-opened LA monomer consisting of two lactate (L) units, trans-esterification reactions can additionally break the ester bond in the lactidyl (LL) unit (as well as the ester bonds between different monomers). Different modes of transesterification, T_{I} (in which the LL unit is preserved) and T_{II} (in which the LL unit is broken and odd numbers of L units are detected), have been defined,[34] although the mechanism of the reaction is the same in each case. Despite transesterification being considered a random process, some dependence on the metal catalyst was observed when the T_{I} and T_{II} modes were first identified.[35] We recently disclosed lanthanum complexes **1–3** (Fig. 1), along with our finding that these catalysts display a high degree of selectivity in transesterification during the copolymerisation of LA and ε-CL.[36] The copolymers are formed *via* a trans-esterification process with both solvent and the number of 2-pyridyl groups in the catalyst found to influence the final copolymer microstructure. Additionally, a complementary, "top-down" controlled transesterification approach has been developed to modify poly(ε-caprolactone)–poly(lactic acid) block copolymers.[37,38] We are interested in developing catalysts with general applicability to cyclic ester copolymerisation, *i.e.* the ability to produce copolymers with the same micro-structure from different monomer pairs. In this contribution, we report the use of **1–3** in the copolymerisation of LA and δ-VL, the characterisation and properties of the resulting copolymers, and the mechanistic insight gained.

Experimental section

Materials

Catalysts **1–3** and all polymers and copolymers were prepared under an inert (nitrogen) atmosphere using standard Schlenk or glovebox (Innovative Technologies) techniques. Dry solvents (toluene, hexane, tetrahydrofuran) were obtained from an Inert SPS (solvent purification system). All solvents and chemicals were purchased from commercial suppliers (Sigma-Aldrich, Strem, Alfa Aesar, TCI) and used as received except where otherwise specified. *Rac*-LA and (*S,S*)-LA were recrystallized once from dry toluene and sublimed once under vacuum at 50 °C. δ-VL was stirred over CaH_2 under N_2 at 50 °C overnight, distilled under vacuum and degassed *via* 3 freeze–pump–thaw cycles. Benzene-d_6 and toluene-d_8 were dried over activated 4 Å molecular sieves and degassed *via* 3 freeze–pump–thaw cycles.
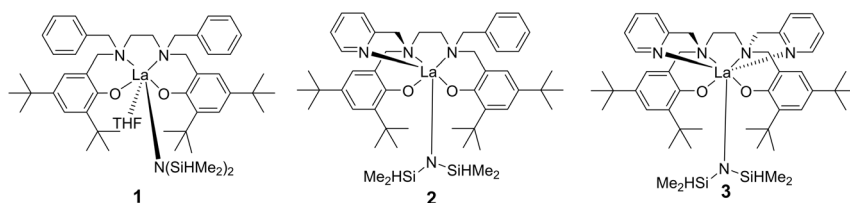

Fig. 1 Structures of **1–3**.

[La(N(SiHMe$_2$)$_2$)$_3$(THF)$_2$],[39] and catalysts **1–3** [36] were prepared following literature procedures.

Methods

^{1}H and ^{13}C NMR spectra were recorded at 400.1 and 100.6 MHz, respectively, on a Bruker Avance III 400 MHz spectrometer equipped with a broadband-observe probe (BBFO). ^{1}H NMR spectra are referenced to residual solvent signals; ^{13}C NMR spectra are referenced to the signal for the solvent ^{13}C nucleus. The temperature was calibrated using deuterated methanol, and unless stated otherwise, were all acquired at 298.0 K. Spectra were processed using either ACD/NMR Processor or Mestrenova 15. Chemical shifts are reported in ppm and coupling constants in Hz. For quantitative ^{13}C NMR experiments, the T_1 of representative poly(VL-co-LA) copolymer samples was measured using inversion recovery experiments. The longest T_1 was determined as 6 seconds. The quantitative 1D ^{13}C spectra were run with inverse-gated decoupling and a relaxation delay of 30 seconds.

Molecular weights of polymers were determined by gel permeation chromatography (GPC) multi-angle laser light scattering (MALLS) in chloroform using a Shimadzu liquid chromatograph equipped with a Shimadzu LC-20AD pump and autosampler, two Phenogel 5 μm linear (2) columns (300 × 7.8 mm), a Shimadzu RID-20A refractive index detector, and a Wyatt miniDAWN TREOS LLS detector. The column temperature was maintained at 40 °C and the flow rate was 1 mL min^{-1}. Samples were dissolved in chloroform at a concentration of 10 mg mL^{-1} and filtered prior to analysis. Data was processed using ASTRA software using dn/dc values of 0.024 and 0.048 for PLA and PVL, respectively.

MALDI-TOF mass spectrometry was conducted at NMSF, Swansea University, UK. Spectra were obtained using a Bruker ultrafleXtreme instrument. The samples were solvated in 100 μL dry THF, mixed at a ratio of 1 : 10 with 20 mg mL^{-1} dithranol matrix in THF with 1 μL NaTFA (to ensure +Na$^+$ adduct ion species) and analysed by positive ion mode in linear and reflectron MALDI.

Differential scanning calorimetry (DSC) measurements were performed using a TA Instruments Q2000 DSC instrument (TA Instruments, Wilmslow UK), equipped with an RCS90 Refrigerated Cooling System (TA Instruments, Wilmslow UK). The instrument was calibrated against an Indium standard, and data were processed using TA Instruments Universal Analysis software. Samples were analysed under a nitrogen atmosphere, in hermetically sealed aluminium TZero crucibles (TA Instruments, Wilmslow, UK). For the analysis of polymer samples, samples were subjected to two heating/cooling cycles, each consisting of: a heating ramp from −80 to 200 °C at a rate of 10 °C min^{-1}, an isothermal phase at 200 °C for 2 minutes, a cooling ramp from 200 °C to −80 °C at a rate of 10 °C min^{-1}, and an isothermal phase at −80 °C for 2 minutes. Glass transition temperatures were recorded as the inflection point and melting points were recorded as the peak value, on the heating phase of the second cycle.

Homopolymerisation of δ-VL

A solution of **1–3** (0.01 mmol) in toluene (0.50 mL) was added to a stirred solution of δ-valerolactone (200 mg, 2.00 mmol) in toluene (1.50 mL) and the mixture left to stir at ambient temperature at a rate of 400 rpm. At a known time the reaction

mixture was removed from the glove box. A few drops of the reaction mixture were added to chloroform (0.80 mL) and this sample analysed by NMR spectroscopy to determine monomer conversion. Hexane was added to the bulk reaction mixture to precipitate the polymer. The crude polymer was dried in a vacuum oven overnight at 60 °C to remove solvents and residual monomer. The polymer was then purified by dissolving it in the minimum volume of chloroform and adding the solution dropwise to methanol with stirring. The precipitated polymer was isolated by vacuum filtration and dried in a vacuum oven overnight at 60 °C.

^{1}H NMR (400 MHz, 298 K, CDCl$_3$): δ 4.08 (m, 2H, OCH_2), 2.36 (m, 2H, CH_2), 1.70 (m, 4H, CH_2) ppm.

^{13}C {^{1}H} NMR (100 MHz, 298 K, CDCl$_3$): δ 173.4 (C=O), 64.1 (OCH$_2$), 33.8 (CH$_2$), 28.2 (CH$_2$), 21.6 (CH$_2$) ppm.

Copolymerisation of LA and δ-VL

A solution of **1–3** (0.01 mmol) in toluene or THF (0.50 mL) was added to a stirred solution of LA (144 mg, 1.00 mmol) and δ-valerolactone (100 mg, 1.00 mmol) in toluene or THF (1.50 mL) and left to stir at ambient temperature at a rate of 400 rpm. At a known time the reaction mixture was removed from the glove box. A few drops of the reaction mixture were added to chloroform (0.80 mL) and this sample analysed by NMR spectroscopy to determine monomer conversion. Hexane was added to the bulk reaction mixture to precipitate the polymer. The crude polymer was dried in a vacuum oven overnight at 60 °C to remove solvents and residual monomer. The polymer was purified by dissolving it in the minimum volume of chloroform and adding the solution dropwise to methanol with stirring. The precipitated polymer was isolated by vacuum filtration and dried in a vacuum oven overnight at 60 °C.

^{1}H NMR (400 MHz, 298 K, CDCl$_3$): δ 5.17–5.06 (m, CH – L unit), 4.13 (m, OCH_2 – VL), 4.06 (m, OCH_2 – VV), 2.42 (m, CH_2 – VL), 2.32 (m, CH_2 – VV), 1.74–1.62 (m, CH_2 × 2 – V unit). 1.57–1.46 (m, CH_3 – L unit) ppm.
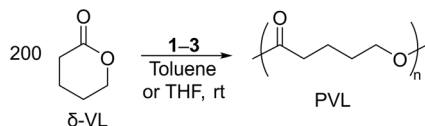
Time-monitored copolymerisation of LA and δ-VL

A solution of **1–3** (0.01 mmol) in toluene or THF (0.50 mL) was added to a stirred solution of LA (144 mg, 1.00 mmol) and δ-valerolactone (100 mg, 1.00 mmol) in toluene or THF (1.50 mL) and stirred at ambient temperature at a rate of 400 rpm. Periodically, aliquots (0.05–0.10 mL) were removed from the reaction mixture and quenched into chloroform (0.80 mL). The solutions were transferred directly to NMR tubes and analysed by ^{1}H NMR spectroscopy using a solvent suppression experiment to determine the monomer conversion. In some cases, the solvent and any residual monomer was removed from each sample by transferring the samples into vials and drying them in a vacuum oven overnight at 60 °C. The residues were dissolved in chloroform-d and analysed by ^{1}H and ^{13}C NMR spectroscopy.

Results and discussion

Homopolymerisation of δ-VL

Lanthanum complexes **1–3** have previously been shown to be highly active in the ROP of *rac*-LA and ε-CL, suggesting that the ROP of δ-VL with these complexes

$$200 \quad \text{δ-VL} \quad \xrightarrow[\substack{\text{Toluene} \\ \text{or THF, rt}}]{\textbf{1–3}} \quad \text{PVL}$$

Scheme 1 Homopolymerisation of δ-VL in toluene or THF catalysed by **1–3**.

would also be rapid. Initially, the ROP of δ-VL was conducted using **1–3** in either THF or toluene, with $[\text{δ-VL}]_0 = 1.0$ M and $[\text{δ-VL}]_0/[\textbf{1–3}] = 200$ (Scheme 1 and Table 1). Monomer conversion was determined by comparison of the integrals of the $\text{OC}H_2$ proton in the monomer and the polymer in ^{1}H NMR spectra of the crude reaction mixtures. Each of the complexes displayed high activity: ≥90% monomer conversions were achieved within 10 min in each case, with higher conversions achieved in toluene compared to THF.

In each case, monomodal GPC traces were obtained. For complexes **1** and **2**, the M_n values are higher than the values calculated from the monomer to catalyst ratio in both toluene and THF, whilst for complex **3**, the M_n values are slightly lower than those calculated. The ROP of δ-VL in THF at a range of catalyst concentrations from $[\text{δ-VL}]_0/[\textbf{3}] = 100–1000$ was explored (Fig. 2). The molecular weights of the polymers increase linearly with $[\text{δ-VL}]_0/[\textbf{3}]$ and are also close to calculated values, with dispersities of 1.23–1.27. When $[\text{δ-VL}]_0/[\textbf{3}] = 1000$, high molecular weight polymer of 83.6 kg mol^{-1} resulted, with no increase in molecular mass distribution. These data demonstrate that **3** is capable of mediating controlled polymerisations of δ-VL.

A low molecular weight sample (Table 1, entry 7) was analysed by matrix-assisted laser desorption-ionisation time-of-flight mass spectrometry (MALDI-ToF MS, Fig. S58†). The spectrum contains a set of signals corresponding to cyclic PVL with no chain ends and there was no evidence of linear polymer end-capped by –N(SiHMe$_2$)$_2$ and –H groups. Similar behaviour has been reported by others and the formation of cyclic polymer is attributed to the intramolecular

Table 1 Homopolymerisation of δ-VL catalysed by **1–3**[a]

Entry	Catalyst	Solvent	$[\text{δ-VL}]_0/$ $[\textbf{1–3}]$	Monomer conversion[b] (%)	$M_n(\text{calc})^{[c]}/$ kg mol^{-1}	$M_n{}^{[d]}/$ kg mol^{-1}	$Đ^{[d]}$
1	**1**	Toluene	200	97	19.4	34.0	1.19
2	**2**	Toluene	200	>99	20.0	35.6	1.23
3	**3**	Toluene	200	>99	20.0	17.6	1.35
4	**1**	THF	200	91	18.2	35.2	1.23
5	**2**	THF	200	91	18.2	27.9	1.22
6	**3**	THF	200	91	18.2	13.9	1.26
7	**3**	THF	100	91	9.1	9.1	1.23
8	**3**	THF	270	91	24.6	20.0	1.25
9	**3**	THF	500	91	45.5	47.2	1.27
10	**3**	THF	1000	91	91.0	83.6	1.24

[a] General polymerisation conditions: $[\text{δ-VL}]_0 = 1.0$ M, rt, 10 min. [b] Determined by ^{1}H NMR spectroscopy. [c] $M_n(\text{calc}) = (100 \times ([\text{δ-VL}]_0/[\text{La}]) \times (\% \text{ conversion δ-VL}/100))$. [d] Number-average molecular weight (M_n) and molecular mass distribution ($Đ = M_w/M_n$) determined by GPC-MALLS at 40 °C in CHCl$_3$ using dn/dc of 0.048 for PVL.
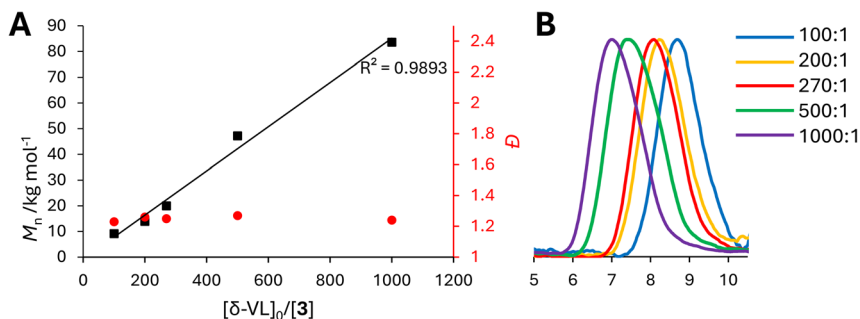
Fig. 2 (A) Plot showing the relationship between M_n of PVL (black squares) and Đ (red circles) with varying $[\delta\text{-VL}]_0/[3]$; (B) GPC traces of PVL at various $[\delta\text{-VL}]_0 : [3]$ ratios.

back-biting reaction of the propagating polymer chain-end at the amide carbonyl.[28,40,41]

Copolymerisation of LA and δ-VL

The behaviour of **1–3** was then explored in the copolymerisation of equimolar amounts of *rac*-LA or *S,S*-LA with δ-VL at ambient temperature, in either THF or toluene, with $[\text{LA}]_0 = [\delta\text{-VL}]_0 = 1.0$ M and $([\text{LA}]_0 + [\delta\text{-VL}]_0)/[\text{La}] = 200$ (Scheme 2 and Table 2). Reactions were quenched by the addition of chloroform to the reaction mixture and ^{1}H NMR spectroscopy of the crude reaction mixture was used to determine monomer conversion. A range of behaviour was observed in terms of activity, M_n of copolymers obtained and copolymer microstructure, demonstrating that the catalyst structure has considerable influence on the copolymers obtained in these reactions.

Much longer reaction times of 2 h are required for maximum conversions of both monomers to be reached in the copolymerisation reaction *vs.* the homo-polymerisation reactions. The conversion of LA reaches complete conversion (>99%) during the reaction time regardless of the catalyst and solvent. In contrast, the conversion of δ-VL is heavily dependent on both the catalyst used and the reaction solvent. With complex **1**, the conversion of δ-VL is limited to <40% in both THF (Table 2, entries 2 and 8) and toluene (entries 1 and 7). With complex **2**, conversions are high in toluene (80–90%, entries 3 and 9), but more modest in THF (entries 4 and 10). Complex **3** is very active and high conversions of δ-VL are achieved in both toluene (>95%, entries 5 and 11) and THF (>85%, entries 6 and 12), although again, the use of THF as reaction solvent does limit the conversion of δ-VL in the reaction. The monomer conversions are reflected in the copolymer compositions: where both monomers reach high conversion the copolymers have close to equimolar compositions, and where the conversion of δ-VL is lower, the
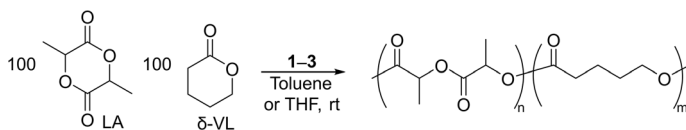
Scheme 2 Copolymerisation of LA and δ-VL in toluene or THF catalysed by **1–3**.

Table 2 Copolymerisation of LA and δ-VL catalysed by **1–3**[a]

Entry	Cat I	LA	Solvent	δ-VL/LA conversion[b] (%)	Composition VL/LA[b] (mol%)	VL–LA/VL–VL[b] (mol%)	l_{LA}/l_{VL}[c]	M_n(calc)[d]/kg mol^{-1}	M_n[e]/kg mol^{-1}	$Đ$[e]
1	**1**	rac-LA	Toluene	18/>99	14/86	43/57	14.3/2.3	8.1	17.4	1.19
2	**1**	rac-LA	THF	16/>99	13/87	57/43	12.4/1.9	8.0	11.2	1.14
3	**2**	rac-LA	Toluene	88/>99	46/54	35/65	3.4/2.9	11.6	8.8	1.18
4	**2**	rac-LA	THF	44/>99	31/69	41/59	5.3/2.4	9.4	11.1	1.14
5	**3**	rac-LA	Toluene	95/>99	47/53	45/55	2.3/2.0	12.0	14.9	1.15
6	**3**	rac-LA	THF	86/>99	46/54	53/47	1.8/2.1	11.5	17.1	1.15
7[f]	**1**	S,S-LA	Toluene	40/>99	29/71	36/64	6.5/2.6	18.4	26.5	1.07
8[f]	**1**	S,S-LA	THF	39/>99	27/73	53/47	5.2/1.9	18.3	20.4	1.22
9[f]	**2**	S,S-LA	Toluene	80/>99	46/54	24/76	4.9/4.2	22.4	21.6	1.31
10[f]	**2**	S,S-LA	THF	41/>99	28/72	40/60	6.5/2.5	18.5	18.5	1.22
11[f]	**3**	S,S-LA	Toluene	97/>99	50/50	35/65	2.9/2.9	24.1	35.2	1.21
12[f]	**3**	S,S-LA	THF	85/>99	45/55	45/55	2.7/2.2	22.9	29.9	1.24

[a] General polymerisation conditions: $[LA]_0 = [δ-VL]_0 = 1.0$ M, $([LA]_0 + [δ-VL]_0)/[La] = 100$, rt, 2 h. [b] Determined from the ^{1}H NMR spectrum. [c] Average sequence length of lactidyl (l_{LA}) and valeroyl (l_{VL}) blocks in the copolymer, determined from the ^{1}H NMR spectrum. [d] M_n(calc) = (100 × 100 × (% conversion δ-VL/100)) + (144 × 100 × (% conversion LA/100)). [e] Number-average molecular weight (M_n) and molecular mass distribution ($Đ = M_w/M_n$) determined by GPC-MALLS at 40 °C in CHCl$_3$ using dn/dc of 0.048 and 0.024 for PVL and PLA, respectively, and dn/dc (copolymer) = (0.048 × weight ratio of VL) + (0.024 × weight ratio of LA). [f] $[LA]_0 + [δ-VL]_0)/[La] = 200$.

incorporation of δ-VL into the copolymer is correspondingly lower. These results demonstrate that both the catalyst structure and the reaction solvent have an impact on δ-VL conversion. High conversions of δ-VL are only achieved when the catalyst possesses at least one 2-pyridyl group and with use of a non-coordinating solvent. The presence of two 2-pyridyl groups reduces the solvent influence on monomer conversion. Since the 2-pyridyl groups on the ligands potentially increase both the electron density at lanthanum and the steric congestion around the metal centre, it is difficult to separate these effects and conclusively attribute the differences in δ-VL reaction to a single facet. Increased electron density at lanthanum from pyridyl group coordination could weaken the putative κ^2-coordination of a ring-opened LA monomer and allow coordination and subsequent reaction of δ-VL. Greater steric congestion around the metal provided by a coordinating 2-pyridyl group could equally hinder κ^2-coordination of the lactate unit at the metal, again potentially facilitating coordination and reaction of δ-VL.

The M_n of the copolymers are in reasonable agreement with values calculated based on the monomer : catalyst ratio, although there is a trend towards higher M_n values, especially with **1** and **3**. The dispersities of 1.07–1.24 are suggestive of controlled polymerisation reactions. The fact that each copolymer displays a monomodal trace when analysed by GPC (Fig. S46–S57†) is strong evidence for the formation of copolymers using **1–3**, rather than the separate homopolymerisation of each monomer. Other evidence that indicates the occurrence of copolymerisation includes ^{1}H DOSY NMR spectra of copolymers prepared with each catalyst show a species with a single diffusion coefficient (Fig. 3, S59 and S60†) and ^{1}H and ^{13}C NMR spectra containing signals assigned to heterodiads and triads (i.e. L units lying next to V units and V units lying next to L units in
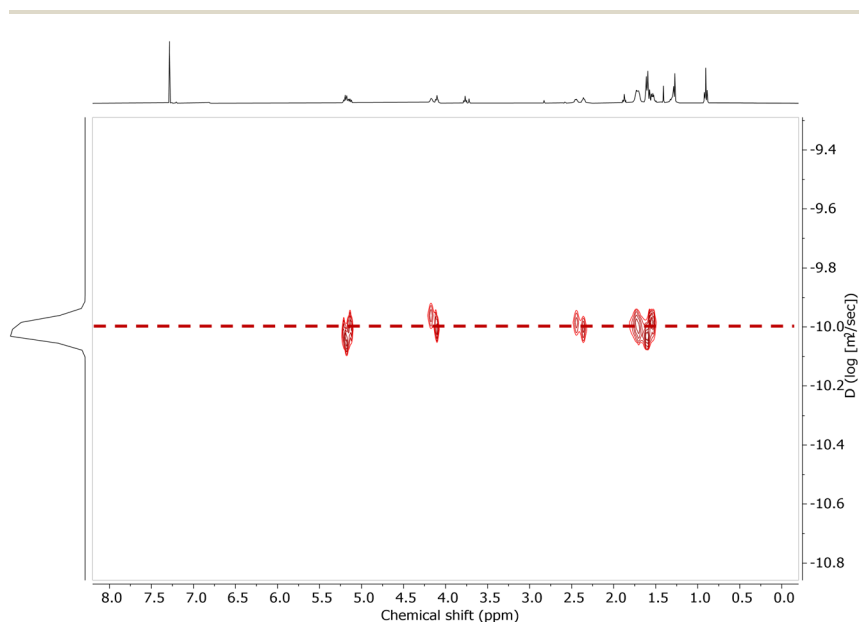

Fig. 3 ^{1}H DOSY NMR spectrum of a poly(lactide-co-valerolactone) copolymer prepared using **3**. Reaction conditions: $[rac\text{-}LA]_0 = [\delta\text{-}VL]_0 = 0.5$ M in THF, $[rac\text{-}LA]_0/\mathbf{3} = 10$, reaction time 20 min.

Faraday Discussions

a copolymer, where L = lactate and V = valeroyl) as well as homodiads and triads. Thus, it is concluded that copolymers are formed in these reactions. MALDI-ToF MS was attempted with copolymers but was unsuccessful.

Copolymer characterisation and microstructure

The ^{1}H NMR spectra of the copolymers were assigned according to literature data (Fig. S1–S12 and S32–S36†).[25] The chemical shift of the *V* unit OCH_2 protons is sensitive to the identity of one adjacent monomer unit (*i.e.* they have diad level sensitivity), giving rise to resonances at 4.08 ppm, assigned to a $\underline{V}V$ unit (*i.e.* a valeroyl unit which lies next to another valeroyl unit) and 4.15 ppm, assigned to a $\underline{V}L$ unit (*i.e.* a valeroyl unit which lies next to a lactate unit, Fig. 4). The relative integration of these signals gives information about the copolymer microstructure. For polymers prepared using complex **1**, the $\underline{V}L$ signal is more intense than the $\underline{V}V$ signal in THF, with the reverse being true when toluene is the solvent (although this is based on a relatively low overall V content in these copolymers). For complex **2** in either solvent and **3** in toluene, $\underline{V}V > \underline{V}L$, and for complex **3** in THF, the proportions of $\underline{V}L$ and $\underline{V}V$ are closer to 50%, indicative of a statistical microstructure (Fig. 5). Interestingly, when *rac*-LA rather than (*S,S*)-LA is used as the comonomer, the proportion of $\underline{V}V$ is lower than $\underline{V}L$ under the same reaction conditions, suggesting use of (*S,S*)-LA leads to copolymers with more block-like microstructures.

Alongside composition, information from the copolymer ^{1}H NMR spectrum allows calculation of the average sequence lengths of valeroyl and lactidyl units, l_{VL} and l_{LA},[42] giving information regarding the microstructure of a copolymer and describing how monomer units are distributed:
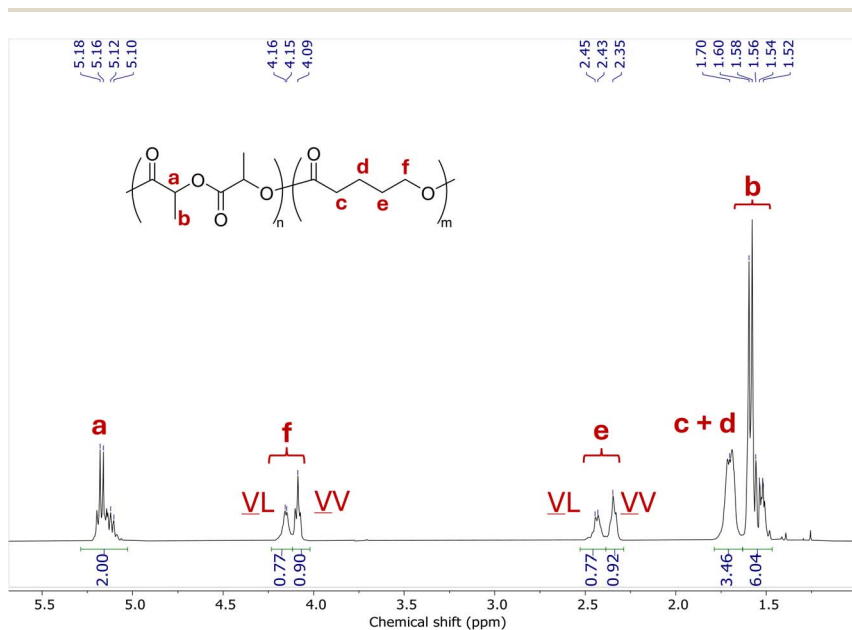

Fig. 4 Assignment of the ^{1}H NMR spectrum of poly(lactide-*co*-valerolactone) copolymer prepared using **3** (Table 2, entry 12). V = valeroyl unit (−C(O)(CH$_2$)$_4$O−), L = lactyl unit (−C(O)CH(CH$_3$)O−), LL = lactidyl unit (−C(O)CH(CH$_3$)OC(O)CH(CH$_3$)O−).
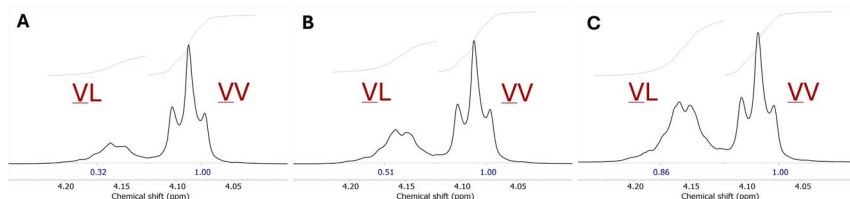
Fig. 5 Comparison of the relative integration of the signals assigned to VL and VV diads in the ^{1}H NMR spectra of poly(lactide-co-valerolactone) copolymers prepared using: (A) **2** in toluene (Table 2, entry 9), (B) **3** in toluene (Table 2, entry 11), (C) **3** in THF (Table 2, entry 12). V = valeroyl unit ($-C(O)(CH_2)_4O-$), L = lactyl unit ($-C(O)CH(CH_3)O-$), LL = lactidyl unit ($-C(O)CH(CH_3)OC(O)CH(CH_3)O-$).

$$l_{VL} = \frac{2(VL)}{(VL - LA)}$$

$$l_{LA} = \frac{2(LA)}{(VL - LA)}$$

High average sequence lengths indicate that monomer units form long sequences of the same type whereas low sequence lengths indicate a high frequency of alternation between monomer unit types and is typical of a high VL–LA diad proportion.

More detailed information about polymer microstructure is obtained from quantitative ^{13}C NMR spectra of copolymers (particularly the carbonyl region), as these provide triad-level data. Whilst the ^{13}C NMR spectra of poly(lactide-co-caprolactone)s have been extensively studied and fully assigned by others, there are very few instances of the ^{13}C NMR spectra of poly(lactide-co-valerolactone)s being reported[43] and, to the best of our knowledge, there is no definitive assignment of the spectrum at 100 MHz to-date. The structural similarity of δ-VL to ε-CL led us to assign the spectrum by comparing the ^{13}C NMR spectra of a poly((S)-lactide-co-caprolactone) and poly((S)-lactide-co-valerolactone) prepared with **3** (Fig. 6), using the literature assignment as a guide.[34] There are four valeroyl-centred signals at 173.4, 173.2, 172.8 and 172.6 ppm, assigned to V_V_V, L_V_V, V_V_L and L_V_L triads, respectively. Signals between 169.5 ppm and 170.4 ppm can be assigned to lactyl-centred triads '*L*' centred triads. There are two additional signals at 170.40 and 170.35 that cannot be mapped onto the current assignment.

For copolymers prepared using catalyst **3**, in which high conversion of δ-VL is achieved, there is a difference in microstructure depending on the solvent used. In THF (Table 2, entry 12), a copolymer with an almost statistical microstructure is formed, as evidenced by the fact that the four V-centred triads have close to equal integration (31 : 22 : 20 : 26). The average sequence lengths of each monomer are calculated from the ^{1}H NMR data as $l_{LA} = 2.7$ and $l_{VL} = 2.2$ when (S,S)-LA is used and $l_{LA} = 1.9$ and $l_{VL} = 2.1$ when *rac*-LA is used (a value of 2 indicates a statistical copolymer). When toluene is the reaction solvent (Table 2, entry 11), the copolymer formed has longer sequences of each monomer, shown by high intensity signals at 173.2 ppm (V_V_V) and 169.6 ppm (LLL_L_LL), accounting for 46% of V-centred signals and 59% of L-centred signals, respectively. Average sequence lengths are $l_{LA} = 2.9$ and $l_{VL} = 2.9$. This behaviour matches that previously
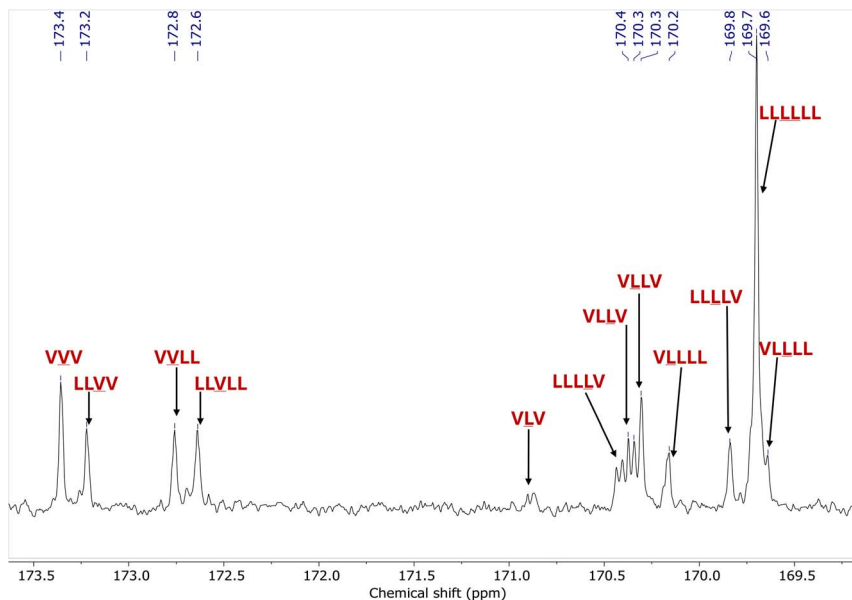
Fig. 6 Carbonyl region in the quantitative ^{13}C NMR spectrum of a poly(lactide-*co*-valerolactone) prepared using **3** in THF (Table 2, entry 12). V = valeroyl unit (−C(O)(CH$_2$)$_4$O−), L = lactyl unit (−C(O)CH(CH$_3$)O−), LL = lactidyl unit (−C(O)CH(CH$_3$)OC(O)CH(CH$_3$)O−).

reported for catalyst **3** in the copolymerisation of LA and ε-CL.[36] In contrast to the previous report, complex **2** produces a copolymer with (*S,S*)-LA and δ-VL in toluene with high intensity homo triad peaks V*V*V = 58% of V-centred triads and LL*LL*LL = 75% of L-centred signals. Average sequence lengths are l_{LA} = 4.9 and l_{VL} = 4.2.

The ^{13}C NMR spectra can also confirm or rule out the occurrence of T_{II} mode of transesterification, since the signal corresponding to the V*L*V triad, which cannot be formed *via* the sequential ROP of LA and δ-VL, is located at 170.8 ppm, in an otherwise empty region of the spectrum.[44] This signal is either not detectable or corresponds to <2% of the total L-centred signals when (*S,S*)-LA is used as the comonomer (Table 2, entries 9–12).

Differences in behaviour of **2** and **3** are observed depending on whether *rac*-LA or (*S,S*)-LA is used. Use of *rac*-LA leads to lower intensity signals for the V*V*V and LL*LL*LL signals in the copolymer ^{13}C NMR spectra compared to when (*S,S*)-LA is used, indicating shorter average sequence lengths. This behaviour has been observed by others in the ROP of LA and ε-CL.[45] Additionally, the V*L*V signal is observed after full monomer conversion, indicating the occurrence of some T_{II} transesterification. However, the peak intensity is low (∼3%). Epimerisation of LA was also observed by **2**, regardless of solvent, evidenced by signals in the ^{13}C NMR spectrum below 169.5 ppm.

Effect of monomer feed ratio on copolymer composition

The copolymerisation of *rac*-LA or *S,S*-LA with δ-VL at various monomer feed ratios was explored, using complex **3** and toluene as solvent (Table 3 and Scheme

Table 3 Copolymerisation of varying ratios of (S,S)-LA and δ-VL catalysed by 3^a

Entry	δ-VL/LA monomer feed (mol%)	δ-VL/LA conv[b] (%)	Composition VL/LA[b] (mol%)	VL–LA/VL–VL[b] (mol%)	l_{LA}/l_{VL}[b]	M_n[c]/kg mol^{-1}	$Đ^c$
1	100/0	95/—	100/0	0/100	—	14.9	1.26
2	20/80	56/>99	12/88	37/63	4.7/0.6	92.6	1.28
3	40/60	87/>99	36/64	37/63	3.5/1.9	39.6	1.27
4	60/40	91/>99	56/44	25/75	3.5/4.5	38.0	1.27
5	80/20	92/>99	79/21	14/86	3.0/11.3	32.8	1.26

^{a} General polymerisation conditions: $[LA]_0 + [δ\text{-}VL]_0 = 1.0$ M in toluene, $([LA]_0 + [δ\text{-}VL]_0)/[3] = 200$, rt, 2 h. ^{b} Determined by ^{1}H NMR spectroscopy. ^{c} Number-average molecular weight (M_n) and molecular mass distribution ($Đ = M_w/M_n$) determined by GPC-MALLS at 40 °C in CHCl$_3$ using dn/dc of 0.048 and 0.024 for PVL and PLA, respectively, and dn/dc (copolymer) = (0.048 × weight ratio of VL) + (0.024 × weight ratio of LA).
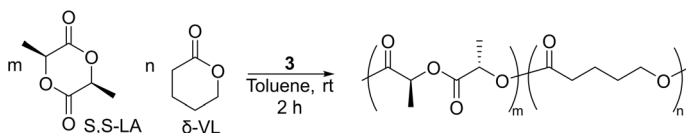
Scheme 3 Copolymerisation of varying ratios of (S,S)-LA and δ-VL in toluene catalysed by **3**.

3). This complex and solvent combination gives the highest monomer conversions of each monomer at an equimolar monomer feed ratio, and therefore a copolymer composition that matches the monomer feed most closely.

Generally the compositions of the copolymers match the monomer feed ratio, except at low $[δ\text{-}VL]_0$ where the reaction mixtures became highly viscous, which severely limits the incorporation of δ-VL into the copolymer. The ratio of $\underline{V}L : \underline{V}V$ appears independent of the $[δ\text{-}VL]_0$ and $\underline{V}V > \underline{V}L$ at all $[δ\text{-}VL]_0$. The value of l_{LA} decreases slightly as $[LA]_0$ and LA mol% decrease, from 4.7 in a copolymer composed of 88% LA (Table 3, entry 2) to 3.0 in a copolymer composed of 21% LA (Table 3, entry 5). In contrast, the value of l_{VL} changes more significantly with changing composition, increasing from 0.6 in a copolymer composed of 12% VL (Table 3, entry 2) to 11.3 in a copolymer composed of 21% LA (Table 3, entry 5).

Thermal properties of copolymers

The thermal properties of some of the copolymers were investigated by differential scanning calorimetry (DSC). Copolymers prepared using **2** and **3** with an equimolar monomer feed (Table 2, entries 9, 11 and 12) and those prepared from variable monomer feed ratios using **3** (Table 3, all entries) were analysed (Table 4 and Fig. S61–S68†). Each of the copolymers displayed a single glass transition (T_g), at a value between that of PLA and PVL, indicative of copolymer formation. There is a linear relationship between LA/VL content and the copolymer T_g. The values for T_g are in reasonable agreement with values calculated using the Fox equation, based on the copolymer compositions (Fig. 7). Copolymers prepared in

Table 4 Thermal properties of poly(lactide-*co*-valerolactone)s with varying compositions[a]

Entry	Catalyst	Reaction solvent	Composition VL/LA (mol%)	T_g/°C	$T_g(\text{calc})^{[b]}$/°C	T_m/°C	ΔH/J g^{-1}
1	**2**	Toluene	46/54	−1.0	5	122.7	0.9
2	**3**	THF	50/50	−1.4	1	—	—
3	**3**	Toluene	45/55	1.1	7	128.7	1.5
4	**3**	Toluene	100/0	—	—	51.4	76.1
5	**3**	Toluene	79/21	−43.4	−30	42.3	2.4
6	**3**	Toluene	56/44	−16.5	−5	127.8	0.2
7	**3**	Toluene	36/64	16.6	17	160.3	25.5
8	**3**	Toluene	12/88	40.6	44	159.8	2.2

[a] Determined using DSC; values obtained from the 2nd heating cycle. A dash indicated the transition was not detected [b] Theoretical T_g value calculated using the Fox equation and copolymer composition.

toluene also displayed melting transitions. For the copolymer with 79% VL content, the T_m of 42.3 °C is close to that of PVL (51.4 °C), suggesting that the crystallinity comes from VL-rich regions of the copolymer. For copolymers with ≤56% VL content, the T_m values lie closer to that of poly(*S*-lactide) (180 °C), suggesting that the crystallinity arises from LA-rich regions of copolymer in these cases. The enthalpies associated with these transitions are low in the copolymers, suggesting a low degree of crystallinity. Overall the DSC data supports the other characterisation data collected, suggesting copolymer formation.

Time-monitored copolymerisation reactions

We have previously determined that **1–3** copolymerise LA and ε-CL *via* a transesterification mechanism.[36] It was of interest to probe the mechanism of copolymerisation with the LA/δ-VL monomer pairing. We hypothesised that a similar mechanism operates, given the similar molecular structures of δ-VL and ε-CL. Polymerisation reactions of equimolar amounts of *rac*-LA and δ-VL in toluene, catalysed by **1–3** at [M]$_0$/[I] 200 were monitored over time through periodic collection of aliquots from the reaction mixture, which were quenched and
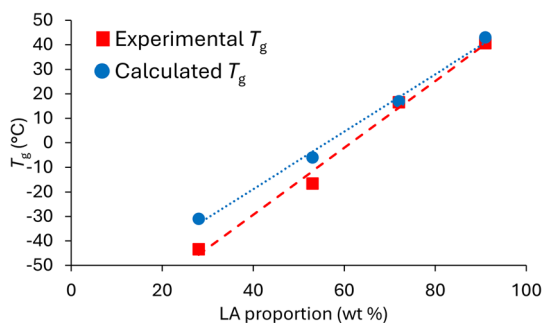

Fig. 7 Plot showing experimental and calculated T_g for poly(lactide-*co*-valerolactone)s prepared using **3** at variable monomer feed ratios.
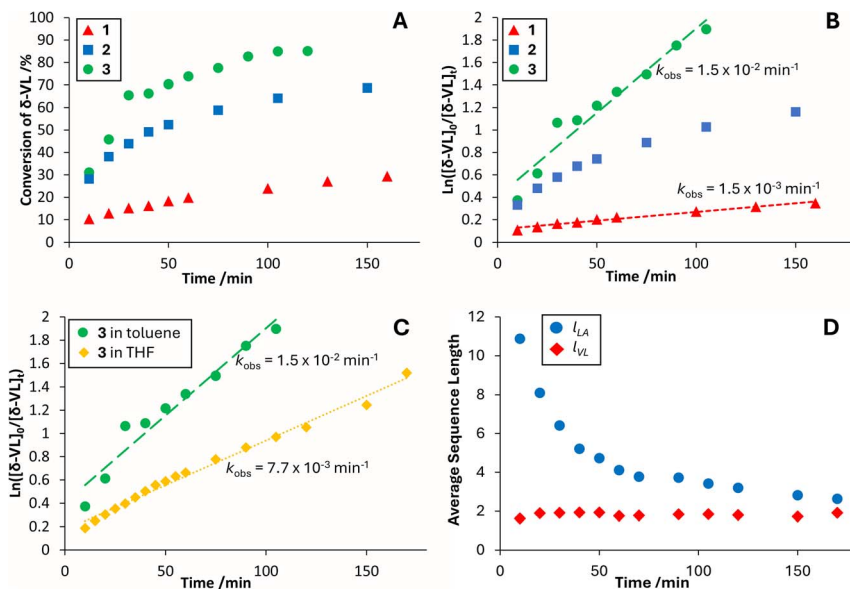
Fig. 8 (A) Plot showing percentage conversion of δ-VL with time (*rac*-LA conversion is at >99% after 5 min) using **1** (red triangle), **2** (blue square) and **3** (green circle) in toluene; (B) semi-logarithmic plot for δ-VL polymerisation using **1** (red triangle), **2** (blue square) and **3** (green circle) in toluene; (C) semi-logarithmic plot for δ-VL polymerisation using **3** in toluene (green circle) and THF (yellow diamond); (D) average sequence length of LA (blue circle) and VL (red diamond) units over time in poly(lactide-*co*-valerolactone) prepared using **3** in THF. Reaction conditions: $[rac\text{-}LA]_0 = [δ\text{-}VL]_0 = 0.5$ M at ambient temperature, $[M]_0/[La] = 200$.

analysed by ^{1}H NMR spectroscopy to determine monomer conversions (Fig. 8A). Within 5 min reaction time, all *rac*-LA is consumed. The δ-VL is then incorporated into the copolymer during the subsequent reaction time.

There are notable differences in the behaviour of each of the catalysts. Firstly, the maximum conversion of δ-VL is ∼30% in the presence of **1**, ∼70% in the presence of **2** and ∼85% in the presence of **3** under the reaction conditions (Fig. 8A). Furthermore, the rate of polymerisation of δ-VL has the order **3** > **2** > **1** (Fig. 8B). A semi-logarithmic plot of the conversion–time data reveals a linear relationship between $\ln([δ\text{-}VL]_0/[δ\text{-}VL]_t)$ and time for **1** and **3**, indicating pseudo first-order kinetic behaviour with respect to [δ-VL] in these cases. However, for **2**, the semi-logarithmic plot deviates quite significantly from linearity. Additionally, a plot of 1/conversion *vs.* time is non-linear, demonstrating that the reaction is not second order with respect to [δ-VL]. Instead, it is proposed that multiple reaction pathways give rise to a fractional power with respect to [δ-VL]. Comparing the reaction rates of **3** in toluene and THF, the rate of δ-VL incorporation into the copolymer is slower in THF, a coordinating solvent ($k_{obs} = 7.7 \times 10^{-3}$ min^{-1}) than in toluene, a non-coordinating solvent ($k_{obs} = 1.5 \times 10^{-2}$ min^{-1}, Fig. 8C). This is attributed to the propensity of THF to bind competitively (but reversibly) to the lanthanum metal centre and prevent/retard coordination of δ-VL monomer to the metal.

Changes to the copolymer microstructure during the reaction were identified by calculation of average sequence lengths from the ^{1}H NMR spectra of the copolymers as the copolymerisation reactions progress (Fig. 8D). These data confirm that the copolymerisation reactions proceed *via* a transesterification mechanism. In the early stages of the reaction, when LA conversion is complete and δ-VL conversion is low, l_{LA} is high (>10). l_{LA} then decreases over the course of 180 minutes. In contrast, l_{VL} stays relatively constant at ∼2 throughout the reaction. After polymer composed of predominantly LL units are formed initially, the V units are incorporated into the polymer chain *via* transesterification. If a block copolymer were formed, l_{LA} would remain constant once fully reacted and l_{VL} would increase as conversion of this monomer increased.

Mechanistic considerations

We have previously established that the copolymerisation of LA and ε-CL mediated by catalysts **2** and **3** proceeds *via* a controlled transesterification mechanism at ambient temperature, with selectivity in the mode of transesterification depending on the number of 2-pyridyl groups installed in the catalyst (1 or 2) and the reaction solvent (coordinating or non-coordinating).[36] It is of interest to compare the behaviour of two different co-monomers and their reactivity with LA. δ-VL (a 6-membered ring lactone) and ε-CL (a seven membered ring lactone) differ only in the inclusion of a CH_2 group in the ring. The homopolymerisation of these monomers has been investigated using La(O^{i}Pr)$_3$[46] and, under the same reaction conditions, the rate of ROP of ε-CL is significantly higher than the rate of ROP of δ-VL (k_{obs}(ε-CL) ≈ 3 × k_{obs}(δ-VL)).[47] Additionally, the ring strain of δ-VL is lower than that of both ε-CL and *rac*-LA.[47]

The microstructure of the copolymer that is produced by each catalyst is dependent on the relative rates of propagation of δ-VL ROP, k_p(VL), in which ring-opening and insertion of δ-VL into the La–OPolymer bond occur (where OPolymer represents the growing polymer chain), and transesterification k_{TE}, in which the ring opening δ-VL monomer unit is immediately incorporated into a PLA polymer block (or a mixed PLA/PVL polymer in the latter stages of the reaction). Where propagation dominates, a more block-like polymer results (if *only* propagation were to occur then a diblock polymer would result). Where transesterification dominates, the outcome is a copolymer with shorter sequence lengths of each monomer units. Given the similarity in structure of ring-opened caproyl and valeroyl units, it would be expected that k_{TE} would be very similar for a given catalyst, regardless of the comonomer identity. A difference in k_p(VL) *vs.* k_p(CL) for a given catalyst would therefore give rise to a difference in copolymer microstructure. Considering the difference in reactivity between δ-VL and ε-CL, it may be expected that, with δ-VL as the comonomer, a lower relative rate of propagation (*vs.* ε-CL) would lead to transesterification reactions dominating, resulting in shorter average sequence lengths. In fact, comparing the average sequence lengths for the LA/ε-CL and LA/δ-VL copolymerisation using **2** and **3**, this outcome is not observed (Table 5). Using complexes **2** and **3** in toluene, poly(lactide-*co*-valerolactone)s have longer average sequence lengths than poly(lactide-*co*-caprolactone)s, with the difference greater for **2** than **3**. On the other hand, using complex **3** in THF, there is almost no difference in average sequence lengths of each unit and statistical copolymers result.

Table 5 Average sequence lengths of monomer units and randomness in poly(lactide-co-caprolactone)s and poly(lactide-co-valerolactone)s prepared with **2** and **3**[a]

Entry	Catalyst	LA isomer	Solvent	Poly(LA-co-CL)		Poly(LA-co-VL)	
				l_{LL}/l_{CL}[b]	R	l_{LL}/l_{VL}[c]	R
1	**2**	rac-LA	Toluene	1.3/1.3	1.6	3.4/2.9	0.6
2	**2**	(S,S)-LA	Toluene	1.2/1.3	1.6	4.9/4.2	0.4
3	**3**	rac-LA	Toluene	2.9/3.8	0.6	2.3/2.0	0.9
4	**3**	(S,S)-LA	Toluene	4.5/4.5	0.4	2.9/2.9	0.7
5	**3**	rac-LA	THF	2.0/1.9	1.0	1.8/2.1	1.0
6	**3**	(S,S)-LA	THF	2.2/2.6	0.9	2.7/2.2	0.8

[a] Calculated from ^{1}H NMR spectra. [b] Calculated from data previously reported.[36] [c] Reproduced from Table 2.

The occurrence of the T_I and T_{II} modes of transesterification also differs between the LA/ε-CL and LA/δ-VL monomer combinations in the case of catalyst **2**. With LA and ε-CL, a high degree of the T_{II} mode of transesterification was observed, leading to a copolymer microstructure intermediate between statistical and alternating, whereas with LA and δ-VL, the copolymers have a much lower R (Table 5, entry 1). The underlying reason for this difference in behaviour is currently unclear, but may relate to the differing structures and thermodynamic parameters of ε-CL and δ-VL.

Conclusions

In summary, we report the one-pot copolymerisation of LA and δ-VL at ambient temperature, using lanthanum catalysts incorporating amine bis(phenolate) ligands, that contain additional 2-pyridyl groups. When tested in δ-VL homo-polymerisation, **1**–**3** rapidly polymerise δ-VL within minutes. In copolymerisation reactions, whilst all catalysts polymerise LA fully, the presence of at least one 2-pyridyl group is crucial to achieve high conversion of δ-VL, with the highest conversions observed with catalyst **3**, containing two 2-pyridyl groups. The reaction solvent (whether coordinating or non-coordinating) also impacts the extent of δ-VL ROP for **2**. Only low conversion of δ-VL is achieved with **1**.

The copolymeric nature of the materials was demonstrated by 1D and 2D NMR spectroscopy, GPC-SEC and DSC. The copolymer microstructure varies, depending on catalyst and the reaction solvent, with the use of THF associated with a more statistical copolymer microstructure, and the use of toluene leading to longer average sequence lengths and more block-like microstructures. It is possible to access the full range of copolymer compositions by varying the monomer feed ratio, and the copolymer composition generally reflects the monomer feed ratio.

The copolymerisation reactions were monitored over time, to investigate the reaction mechanism. The LA is consumed rapidly during the early stages of the reaction (∼5 min), with the δ-VL conversion then occurring over the rest of the reaction time. The fact that block copolymers are not formed demonstrates that a transesterification mechanism operates. Both the maximum conversion of δ-VL and the pseudo-first order rate constants (k_{obs}) are in the order **3** > **2** > **1**. It is

shown that the transesterification is selective, with very little evidence for the T_{II} mode occurring with (S,S)-LA, leading to copolymers with LL units preserved. It is notable that this transesterification occurs at ambient temperature. Overall this study shows that this catalyst family, particularly **3**, is competent in the ROP of LA with δ-VL, to deliver copolymers with diverse microstructures, that are prepared under mild conditions.

Data availability

The data supporting this article have been included as part of the ESI.†

Conflicts of interest

There are no conflicts to declare.

Acknowledgements

References

1 M. S. Kim, H. Chang, L. Zheng, Q. Yan, B. F. Pfleger, J. Klier, K. Nelson, E. L. W. Majumder and G. W. Huber, *Chem. Rev.*, 2023, **123**, 9915–9939.

2 C. Shi, E. C. Quinn, W. T. Diment and E. Y. X. Chen, *Chem. Rev.*, 2024, **124**, 4393–4478.

3 C. V. Aarsen, A. Liguori, R. Mattsson, M. H. Sipponen and M. Hakkarainen, *Chem. Rev.*, 2024, **124**, 8473–8515.

4 F. M. Haque, J. S. A. Ishibashi, C. A. L. Lidston, H. Shao, F. S. Bates, A. B. Chang, G. W. Coates, C. J. Cramer, P. J. Dauenhauer, W. R. Dichtel, C. J. Ellison, E. A. Gormong, L. S. Hamachi, T. R. Hoye, M. Jin, J. A. Kalow, H. J. Kim, G. Kumar, C. J. Lasalle, S. Liffland, B. M. Lipinski, Y. Pang, R. Parveen, X. Peng, Y. Popowski, E. A. Prebihalo, Y. Reddi, T. M. Reineke, D. T. Sheppard, J. L. Swartz, W. B. Tolman, B. Vlaisavljevich, J. Wissinger, S. Xu and M. A. Hillmyer, *Chem. Rev.*, 2022, **122**, 6322–6373.

5 A. Sangroniz, J. B. Zhu, X. Tang, A. Etxeberria, E. Y. X. Chen and H. Sardon, *Nat. Commun.*, 2019, **10**, 3559.

6 M. Rabnawaz, I. Wyman, R. Auras and S. Cheng, *Green Chem.*, 2017, **19**, 4737–4753.

7 S. Farah, D. G. Anderson and R. Langer, *Adv. Drug Delivery Rev.*, 2016, **107**, 367–392.

8 R. H. Platel, L. M. Hodgson and C. K. Williams, *Polym. Rev.*, 2008, **48**, 11–63.

9 H. R. Kricheldorf, T. Mang and J. M. Jonté, *Macromolecules*, 1984, **17**, 2173–2181.

10 H. R. Kricheldorf, M. Berl and N. Scharnagl, *Macromolecules*, 1988, **21**, 286–293.

11 P. H. Dubois, I. Barakat, R. Jérême and P. H. Teyssié, *Macromolecules*, 1993, **26**, 4407–4412.

12 E. Castro-Aguirre, F. Iñiguez-Franco, H. Samsudin, X. Fang and R. Auras, *Adv. Drug Delivery Rev.*, 2016, **107**, 333–366, DOI: 10.1016/j.addr.2016.03.010.

13 X. Pang, X. Zhuang, Z. Tang and X. Chen, *Biotechnol. J.*, 2010, **5**, 1125–1136.

14 M. J. Stanford and A. P. Dove, *Chem. Soc. Rev.*, 2010, **39**, 486–494.

15 Y. Ikada, K. Jamshidi, H. Tsuji and S. H. Hyon, *Macromolecules*, 1987, **20**, 904–906.

16 H. Tsuji, *Adv. Drug Delivery Rev.*, 2016, **107**, 97–135.

17 T. Rosen, I. Goldberg, V. Venditto and M. Kol, *J. Am. Chem. Soc.*, 2016, **138**, 12041–12044.

18 E. Stirling, Y. Champouret and M. Visseaux, *Polym. Chem.*, 2018, **9**, 2517–2531.

19 M. Aubin and R. E. Prud'homme, *Polymer*, 1981, **22**, 1223–1226.

20 N. Kasyapi and A. K. Bhowmick, *RSC Adv.*, 2014, **4**, 27439–27451.

21 Y. Huang, R. Chang, L. Han, G. Shan, Y. Bao and P. Pan, *ACS Sustainable Chem. Eng.*, 2016, **4**, 121–128.

22 A. Nakayama, N. Kawasaki, S. Aiba, Y. Maeda, I. Arvanitoyannis and N. Yamamoto, *Polymer*, 1998, **39**, 1213–1222.

23 T. R. Panthani and F. S. Bates, *Macromolecules*, 2015, **48**, 4529–4540.

24 J. Fernández, A. Larrañaga, A. Etxeberria and J. R. Sarasua, *J. Mech. Behav. Biomed. Mater.*, 2014, **35**, 39–50.

25 A. Sangroniz, L. Sangroniz, S. Hamzehlou, N. Aranburu, H. Sardon, J. R. Sarasua, M. Iriarte, J. R. Leiza and A. Etxeberria, *Polymers*, 2022, **14**, 52.

26 D. J. Darensbourg, O. Karroonnirun and S. J. Wilson, *Inorg. Chem.*, 2011, **50**, 6775–6787.

27 Y. Nakayama, K. Sasaki, N. Watanabe, Z. Cai and T. Shiono, *Polymer*, 2009, **50**, 4788–4793.

28 X. L. Li, R. W. Clarke, H. Y. An, R. R. Gowda, J. Y. Jiang, T. Q. Xu and E. Y. X. Chen, *Angew. Chem., Int. Ed.*, 2023, **62**, e202303791.

29 P. Nanthananon and Y. K. Kwon, *Green Chem.*, 2024, **26**, 2031–2043.

30 D. J. Gilmour, R. L. Webster, M. R. Perry and L. L. Schafer, *Dalton Trans.*, 2015, **44**, 12411–12419.

31 R. L. Webster, N. Noroozi, S. G. Hatzikiriakos, J. A. Thomson and L. L. Schafer, *Chem. Commun.*, 2012, **49**, 57–59.

32 H. Ouyang, D. Yuan, K. Nie, Y. Zhang, Y. Yao and D. Cui, *Inorg. Chem.*, 2018, **57**, 9028–9038.

33 J. Shao, H. Zhou, Y. Wang, Y. Luo and Y. Yao, *Dalton Trans.*, 2020, **49**, 5842–5850.

34 J. Kasperczyk and M. Bero, *Makromol. Chem.*, 1991, **192**, 1777–1787.

35 M. Bero, J. Kasperczyk and G. Adamus, *Makromol. Chem.*, 1993, **194**, 907–912.

36 B. Beament, D. Britton, T. Malcomson, G. R. Akien, N. R. Halcovitch, M. P. Coogan and R. H. Platel, *Inorg. Chem.*, 2024, **63**, 280–293.

37 M. Abdul Rahman, T. J. Neal and J. A. Garden, *Chem. Commun.*, 2024, **60**, 5530–5533.

38 T. J. Neal, E. D. Neal, J. Cumby and J. A. Garden, *Polym. Chem.*, 2024, **15**, 1704–1713.

39 W. A. Herrmann, F. C. Munck, G. R. J. Artus, O. Runte and R. Anwander, *Organometallics*, 1997, **16**, 682–688.

40 A. Amgoune, C. M. Thomas, S. Ilinca, T. Roisnel and J.-F. Carpentier, *Angew. Chem., Int. Ed.*, 2006, **45**, 2782–2784.

41 M. Hong and E. Y. X. Chen, *Nat. Chem.*, 2015, **8**(1), 42–49.

42 I. R. Herbert, in *NMR Spectroscopy of Polymers*, ed. R. N. Ibbett, Springer Netherlands, 1993, pp. 50–79.

43 H. Fukuzaki, M. Yoshida, M. Asano, Y. Aiba and I. Kaetsu, *Eur. Polym. J.*, 1988, **24**, 1029–1036.

44 J. Kasperczyk and M. Bero, *Makromol. Chem.*, 1993, **194**, 913–925.

45 M. Bero and J. Kasperczyk, *Macromol. Chem. Phys.*, 1996, **197**, 3251–3258.

46 M. Save and A. Soum, *Macromol. Chem. Phys.*, 2002, **203**, 2591–2603.

47 M. Save, M. Schappacher and A. Soum, *Macromol. Chem. Phys.*, 2002, **203**, 889–899.